AGU PUBLICATIONS

Geophysical Research Letters

RESEARCH LETTER
10.1002/2016GL070741

**Key Points:**
- Vegetation exerted a first-order control on landslide initiation location during an extreme rainfall event
- Landslide initiation was controlled by variations in apparent cohesion due to roots rather than interception or bedrock permeability
- Climate change could substantially influence landslide hazards throughout semiarid portions of the southwestern U.S.

**Correspondence to:**
L. A. McGuire,
lmcguire@email.arizona.edu

**Citation:**
McGuire, L. A., F. K. Rengers, J. W. Kean, J. A. Coe, B. B. Mirus, R. L. Baum, and J. W. Godt (2016), Elucidating the role of vegetation in the initiation of rainfall-induced shallow landslides: Insights from an extreme rainfall event in the Colorado Front Range, *Geophys. Res. Lett.*, *43*, 9084–9092, doi:10.1002/2016GL070741.

Received 20 MAY 2016
Accepted 26 AUG 2016
Accepted article online 4 SEP 2016
Published online 14 SEP 2016



# Elucidating the role of vegetation in the initiation of rainfall-induced shallow landslides: Insights from an extreme rainfall event in the Colorado Front Range

**Luke A. McGuire[1,2], Francis K. Rengers[1], Jason W. Kean[1], Jeffrey A. Coe[1], Benjamin B. Mirus[1], Rex L. Baum[1], and Jonathan W. Godt[1]**

[1]U.S. Geological Survey, Denver, Colorado, USA, [2]Department of Geosciences, University of Arizona, Tucson, Arizona, USA

**Abstract** More than 1100 debris flows were mobilized from shallow landslides during a rainstorm from 9 to 13 September 2013 in the Colorado Front Range, with the vast majority initiating on sparsely vegetated, south facing terrain. To investigate the physical processes responsible for the observed aspect control, we made measurements of soil properties on a densely forested north facing hillslope and a grassland-dominated south facing hillslope in the Colorado Front Range and performed numerical modeling of transient changes in soil pore water pressure throughout the rainstorm. Using the numerical model, we quantitatively assessed interactions among vegetation, rainfall interception, subsurface hydrology, and slope stability. Results suggest that apparent cohesion supplied by roots was responsible for the observed connection between debris flow initiation and slope aspect. Results suggest that future climate-driven modifications to forest structure could substantially influence landslide hazards throughout the Front Range and similar water-limited environments where vegetation communities may be more susceptible to small variations in climate.

## 1. Introduction

Forest structure within the southwestern United States, and perhaps more generally in water-limited areas across the world, could change dramatically within the 21st century as a result of changing climatic conditions [*Williams et al.*, 2013]. Changes in vegetation have the potential to substantially modify hydrologic and geomechanical properties on hillslopes that control slope stability. For example, vegetation influences slope stability indirectly through interception [e.g., *Wilkinson et al.*, 2002; *Keim and Skaugset*, 2003], which changes the total volume and timing at which rainfall reaches the soil surface and potentially by increasing the effective permeability in the underlying bedrock via root penetration. The root network can also directly contribute to an apparent cohesion that stabilizes the soil [e.g., *Gray and Megahan*, 1981; *Schmidt et al.*, 2001]. Variations in slope stability conferred by vegetation have immediate impacts on landslide hazards and may also affect erosion rates and soil thickness in steep landscapes over longer timescales by influencing the amount of sediment transported by debris flows [e.g., *Gabet and Dunne*, 2002]. To accurately assess the rate and magnitude at which future shifts in vegetation type and density will affect landslide hazards and sediment transport on steep hillslopes, it is necessary to better quantify the role of vegetation in stabilizing hillslopes during extreme rainfall events.

In September 2013, a large rainfall event struck the northern Colorado Front Range over a period of 5 days (9–13 September 2013), during which a historic amount of precipitation fell on the Front Range foothills, in and around Boulder, CO. Detailed mapping from satellite imagery has identified 1138 debris flows that were mobilized from shallow landslides [*Coe et al.*, 2014]. Debris flows were observed along a wide swath of the Colorado Front Range, across an elevation gradient ranging from 1700 m to 4000 m and in regions with cumulative rainfall totals ranging from 50 mm to 300 mm [*Coe et al.*, 2014]. However, 78% of debris flows initiated on slopes with a south facing aspect [*Coe et al.*, 2014]. In the Colorado Front Range, as well as in many other semiarid environments, differences in ecosystem communities [*Marr*, 1961; *Veblen and Donnegan*, 2005] and soil development [*Birkeland et al.*, 2003] can vary substantially on opposing hillslope aspects due to differences in solar radiation. Because vegetation communities can vary with aspect over very small (<1 km) spatial scales

within the Colorado Front Range, this storm provided a natural experiment to quantify the relative importance of different interactions among vegetation and slope stability in a localized study area where rainfall can be considered relatively uniform.

Understanding the underlying physical processes responsible for the apparent aspect-related control on debris flow initiation would provide valuable insight into the relative importance of different factors in determining future landslide hazards. Particularly in water-limited environments, microclimatic differences between opposing north and south facing hillslopes can be strong enough to influence the development of soil and bedrock properties over geologic timescales [e.g., *Rech et al.*, 2001; *Birkeland et al.*, 2003; *Befus et al.*, 2011; *Burnett et al.*, 2008], which can, in turn, affect the spatial distribution of debris flow initiation locations. To date, several different hypotheses based on slope aspect-driven variations in soil and bedrock properties have been proposed to explain the observed spatial pattern in landslide locations throughout the Colorado Front Range but none have been quantitatively tested. *Coe et al.* [2014] speculate that thinner soils on south facing slopes may be a potential reason for preferential triggering of debris flows on those slopes. *Ebel et al.* [2015] suggested that the increased prevalence of debris flows on south facing hillslopes could be attributed to increased bedrock permeability on north facing hillslopes, relative to south facing hillslopes, that prevented soils on those slopes from becoming saturated. In a recent study, however, *Rengers et al.* [2016] demonstrated that landslide initiation points correspond with present-day locations that have a low vegetation density regardless of slope aspect. Still, given that vegetation can influence slope stability by intercepting rainfall, modifying bedrock properties via root-driven mechanical weathering, or by providing apparent soil cohesion, the underlying physical cause(s) that led to the observed pattern between debris flow initiation and slope aspect remains unexplained.

In this study, we use a combination of field measurements, laboratory analyses, and numerical modeling of slope stability to test the above hypotheses that explain the stability of vegetated, north facing slopes relative to less-vegetated, south facing slopes. In addition, we perform a series of numerical model simulations to isolate the importance of the hydrologic effects of vegetation relative to its geomechanical effects during the studied rainstorm. In particular, we test the hypotheses that greater landslide densities on south facing relative to north facing slopes resulted from (1) the presence of thinner soils on south facing slopes, (2) increased bedrock weathering, and therefore increased bedrock permeability, on north facing slopes, (3) increased rainfall interception on north facing slopes, and (4) increased root reinforcement on north facing slopes.

## 2. Study Area

This study focused on a 0.25 $km^2$ area adjacent to the North Saint Vrain Creek near Allenspark, CO (Figure 1). The study area, located at approximately 2300–2500 m in elevation, lies within the montane ecological zone [*Veblen and Donnegan*, 2005] and is underlain by granitic rocks [*Green*, 1992]. North facing hillslopes are covered by a dense forest of ponderosa pine (*Pinus ponderosa*) and Douglas fir (*Pseudotsuga menziesii*) while south facing hillslopes support grass with a few small shrubs (Figure 1). Fifteen debris flows were mobilized from shallow landslides in the portion of the study area consisting of south facing slopes greater than >25° (0.12 $km^2$). Only two debris flows occurred on the corresponding north facing slope, which equates to a landslide density of 54 landslides/ $km^2$ (roughly 2.5 times lower than the density on the south facing slope) when only considering the area with slope angles above 25°.

## 3. Methods

### 3.1. Numerical Model

Numerical modeling of subsurface flow was performed using Hydrus-1D [*Šimunek et al.*, 2005]. Hydrus-1D, which solves Richards equation within a one-dimensional soil column, was used to compute the time-varying pressure head and moisture content in response to rainfall throughout the storm event. Input parameters for the numerical model are based on in situ measurements made at the field site, laboratory analyses of soil samples, and values obtained from the literature as described in more detail in section 3.2. The model domain consists of a homogeneous layer of soil (constrained by field measurements) underlain by a uniform layer of bedrock, which extends down to a depth of 3 m and is allowed to drain in the vertical direction. We assume that any downslope drainage of water out of the one-dimensional soil column is compensated for by upslope water input. We chose the Hydrus-1D model because it is complex enough to represent the essential processes (transient changes in pore pressure within variably saturated soil), is capable of ingesting

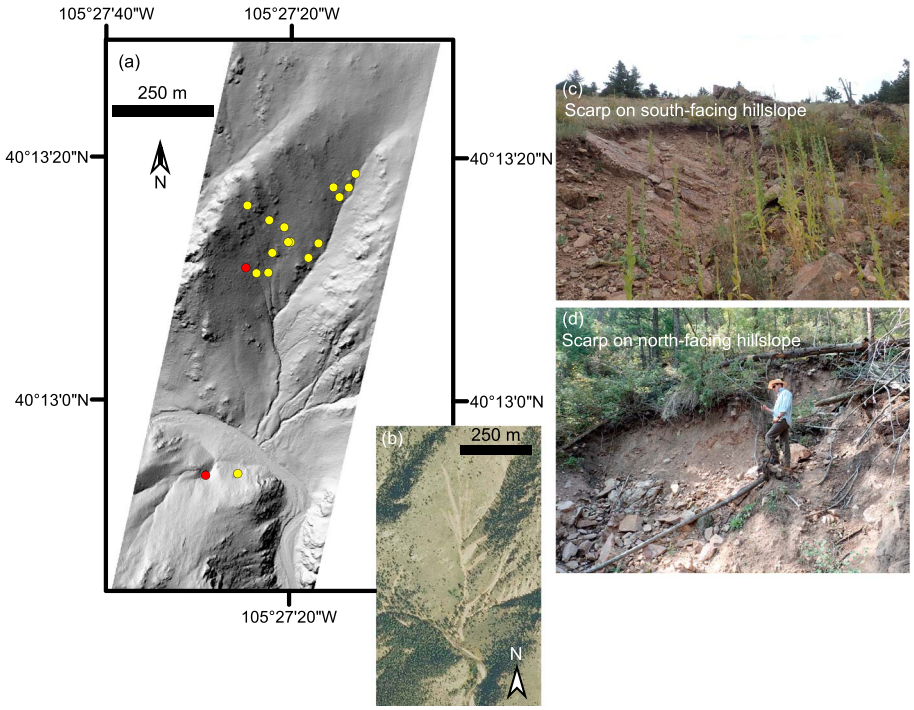


**Figure 1.** (a) The study area is located several miles northeast of Allenspark, CO, at an elevation of approximately 2300–2500 m. Landslide locations are marked by dots, with red dots indicating the locations of two scarps where soil samples were taken for geotechnical analyses. (b) South facing hillslopes support grass and shrubs while north facing hillslopes are heavily forested. (c) Photographs looking upslope at a typical landslide scarp on the south facing hillslope and (d) the north facing hillslope.

the field measurements as input data, and simple enough that there are not a large number of unconstrained parameters.

We assessed slope stability using an infinite slope stability model, or the ratio of the net downslope driving force to the resisting force holding the soil column in place assuming an infinite slope with a constant gradient, given by *Lu and Godt* [2008]

$$F_s = \frac{\tan\phi}{\tan\theta_t} + \frac{2C}{\gamma_s h \sin 2\theta_t} - \frac{\sigma_s}{\gamma_s h}\left(\tan\theta_t + \cot\theta_t\right)\tan\phi \tag{1}$$

A factor of safety ($F_s$) below 1 indicates that the slope is unstable. Here $\theta_t$ denotes the topographic slope angle, $C = C_s + C_v$ is the bulk cohesion, $C_s$ is the cohesion attributable to soil properties, $C_v$ is the cohesion attributable to roots, $h$ is soil thickness, $\gamma_s$ is the unit weight of the soil, and $\phi$ is the friction angle. Letting $\theta_s$ denote soil water content at saturation, $\theta_r$ the residual soil water content, $\gamma_w$ the unit weight of water, and $\psi$ the pressure head, the suction stress ($\sigma_s$) is defined as

$$\sigma_s = \frac{\theta - \theta_r}{\theta_s - \theta_r}\psi\gamma_w \tag{2}$$

Cohesion attributable to roots, $C_v$, is estimated at our study area based on previously published data for the relevant vegetation type. The basal reinforcement due to grass, which dominates on the south facing portion of the study area, is approximately 1.6–2.1 kPa [*Schmidt et al.*, 2001], whereas values in the range $C_v \approx 2.8$–6.2 kPa [*Gray and Megahan*, 1981] are more appropriate for the pine and fir forest on the north facing hillslope. We use the mean slope angles for north and south facing hillslopes at our study site, $\theta_t = 32°$ and $\theta_t = 28°$, respectively, as representative slope angles to compute the factor of safety.

Fifteen minute rainfall intensity ($R$) during the storm was computed using data from the rain gage at Big Elk Park, operated by the Urban Drainage and Flood Control District, located approximately 2 km from the study site. To account for interception from the dense forest on the north facing hillslope, the effective rainfall rate ($R_i$) was computed using the Rutter interception model [*Rutter et al.*, 1972, 1975],

$$R_i = pR + D \tag{3}$$

where $p$ is the throughfall coefficient, $D = \kappa \exp(g(\beta - S))$ is the rate at which water drains from the canopy, $\beta$ is the amount of water stored in the canopy, $S$ is the canopy capacity, and $g = 3.9\ \mathrm{mm}^{-1}$ and $\kappa = 5 \cdot 10^{-8}\ \mathrm{m\ s}^{-1}$ are empirical coefficients. Based on best fit values obtained by *Rutter et al.* [1972, 1975] for a pine forest, we let $p = 0.25$ and $S = 1.05$ mm. As it rains, the amount of water stored in the canopy varies with time ($t$) according to

$$\frac{\partial \beta}{\partial t} = (1 - p)R - D - \frac{\beta}{S}E \tag{4}$$

where $E \approx 0.6\ \mathrm{mm\ h}^{-1}$ is the evaporation rate, computed using meteorological data from the Denver International Airport and an approximation to the Penman equation [*Teklehaimanot and Jarvis*, 1991].

To explore the various ways in which vegetation may have increased the stability of the north facing hillslope at our study area relative to the south facing hillslope, we performed model simulations for several different scenarios. On north facing hillslopes, we assessed the relative importance of interception by performing model experiments using the unmodified rainfall intensity, $R$, as well as $R_i$ as input. Similarly, we examined the impact of bedrock weathering on the north facing hillslope by modifying the values for saturated hydraulic conductivity, $k_{sb}$, and soil moisture content at saturation, $\theta_{sb}$, within the bedrock layer to be consistent with varying degrees of weathered granitic rock. In particular, based on the values measured by *Katsura et al.* [2009], we let $k_{sb} = 10^{-6}\ \mathrm{m\ s}^{-1}$ and $\theta_{sb} = 0.2$ represent highly weathered bedrock and let $k_{sb} = 10^{-9}\ \mathrm{m\ s}^{-1}$ and $\theta_{sb} = 0.15$ represent relatively unweathered bedrock. Lastly, we isolate the impact of apparent root cohesion on slope stability by comparing model results with and without including apparent cohesion due to root reinforcement in the factor of safety calculation.

Since there is minimal vegetation on the south facing hillslope relative to the north facing hillslope, we did not perform the same sensitivity analysis for the south facing hillslope. For model experiments on the south facing hillslope, we assume that interception is negligible and that there is a small amount of root reinforcement, consistent with the presence of grass and shrubs. However, since bedrock permeability is an unknown at our study area, we assessed its potential influence on slope stability on the south facing hillslope by varying $k_{sb}$ and $\theta_{sb}$ in the bedrock layer as was done with the simulations for the north facing slope.

We performed model simulations using inputs for soil thickness ($h$) and soil saturated hydraulic conductivity ($k_s$) that are given by the mean of the values measured in the field for north and south facing hillslopes. To assess uncertainty in the model solution, we performed simulations for all of the different modeling scenarios using saturated hydraulic conductivities and soil thickness values corresponding to the lower ($Q_1$) and upper ($Q_3$) quartile values of the measurements. By varying soil thickness within the simulations, we were also able to assess the role of soil thickness in contributing to the prevalence of landslides on the south facing hillslope.

### 3.2. Field Measurements and Laboratory Analyses

Input parameters for the numerical model were constrained from field measurements of soil thickness and saturated hydraulic conductivity, as well as laboratory measurements of particle size distributions and soil strength. We made estimates of soil thickness at landslide locations by measuring the depth to the failure plane, which corresponded to the bedrock interface in all cases. Measurements of soil thickness on both hillslopes were supplemented by excavating pits (over an area approximately 1 m by 1 m) to the point of refusal and also by drilling to bedrock with a portable backpack drill. A total of 18 and 11 soil thickness measurements were made on the south and north facing portions of the study area, respectively.

Infiltration measurements were made near soil pit locations using a tension infiltrometer after brushing away any surface litter, yielding 17 measurements on the south facing hillslope and 17 on the north facing hillslope. The cumulative volume infiltrated was recorded as a function of time and then used to calculate the saturated hydraulic conductivity following the methodology of *Zhang* [1997].

The internal friction angle and apparent soil cohesion ($C_s$) were obtained from the results of torsional ring shear tests performed using sediment samples taken from one scarp on the south facing hillslope and one scarp on the north facing hillslope. Soil samples used for geotechnical analyses were taken approximately halfway between the failure plane and the surface. Soil texture information was obtained through particle size analysis of samples taken from the surface and from halfway between the surface and the bedrock interface.

**Table 1.** Model Parameter Values Used in Numerical Simulations of Subsurface Flow and Slope Stability at the North Saint Vrain Study Site[a]

| Symbol | Unit | Definition | Value (North) | Value (South) | Source |
|---|---|---|---|---|---|
| $h$ | m | Mean soil thickness | 0.64 | 0.56 | M |
| $k_s$ | m s$^{-1}$ | Saturated hydraulic conductivity | $5.83 \cdot 10^{-6}$ | $1.53 \cdot 10^{-5}$ | M |
| $\theta_s$ | - | Saturated volumetric water content | 0.41 | 0.41 | L |
| $\theta_r$ | - | Residual volumetric water content | 0.065 | 0.065 | L |
| $\alpha$ | m$^{-1}$ | Parameter in soil water retention function | 7.5 | 7.5 | L |
| $n$ | - | Exponent in soil water retention function | 1.89 | 1.89 | L |
| $\phi_s$ | deg | Static angle of friction for sediment | 31 | 29 | M |
| $C_s$ | kPa | Apparent cohesion in absence of roots | 0 | 0 | M |
| $C_v$ | kPa | Apparent cohesion from vegetation | 2.8–6.2 | 1.6–2.1 | L |
| $\theta_t$ | deg | Representative hillslope angle | 32 | 28 | M |
| $k_{sb}$ | m s$^{-1}$ | Saturated hydraulic conductivity (bedrock) | $10^{-6}$–$10^{-9}$ | $10^{-6}$–$10^{-9}$ | L |
| $\theta_{sb}$ | - | Saturated volumetric water content (bedrock) | 0.15–0.2 | 0.15–0.2 | L |

[a]The letters L and M refer to values that were inferred from the literature and derived from measurements or laboratory analyses of sediment from our study site, respectively. Values for $\theta_s$, $\alpha$, and $n$ were obtained from *Carsel and Parrish* [1988], values for $C_v$ are from *Schmidt et al.* [2001] and *Gray and Megahan* [1981], and ranges for $k_{sb}$ and $\theta_{sb}$ are from *Katsura et al.* [2009].

## 4. Results

Soil properties vary between the north and south facing hillslopes within our study area (Table 1) but are qualitatively similar in many ways. Soils on both hillslopes are shallow, gravelly, and show little signs of horizonation. Mean soil thickness on the south facing hillslope is 0.56 m, with an interquartile range of 0.43–0.61 m, compared with a mean of 0.64 m and an interquartile range of 0.48–0.73 m on the corresponding north facing hillslope. North facing hillslopes typically have several centimeters of surface litter and dark organic matter. Based on the particle size distributions obtained near the surface and halfway between the surface and the bedrock interface, soils on north and south facing hillslopes can be classified as sandy loams.

Soils on the north facing hillslope have a mean saturated hydraulic conductivity of $k_s = 21$ mm h$^{-1}$ with an interquartile range of 11–24 mm h$^{-1}$. Saturated hydraulic conductivities on south facing hillslopes are higher, having a mean of $k_s = 55$ mm h$^{-1}$ and an interquartile range of 30–86 mm h$^{-1}$. Torsional ring shear tests revealed that soils on the north facing hillslope have a friction angle of $\phi = 31 \pm 1°$, slightly higher than the value of $\phi = 29 \pm 1°$ on the south facing hillslope. Soils on both hillslopes have negligible soil cohesion (i.e., $C_s = 0$).

Numerical model results are consistent with observations at our study area of widespread landslide initiation on the south facing hillslope and only two landslides on the north facing hillslope. On the south facing slope, the model-simulated factor of safety decreases over time to a value less than 1, indicating that the soil column becomes unstable (Figure 2b, black lines). A model sensitivity analysis revealed that simulated south facing slopes become unstable for a wide range of soil depths (from $Q_1 = 0.43$ to $Q_3 = 0.61$ m) and saturated hydraulic conductivities (from $Q_1 = 30$ to $Q_3 = 86$ mm h$^{-1}$). The simulated factor of safety corresponding to the most and least stable of the above cases with variable soil thickness and saturated hydraulic conductivities are presented in Figure 2 (gray lines). In contrast, the simulated factor of safety on the north facing hillslope is always greater than 1, indicating stable conditions, when cohesion from the root network is included in the calculation (Figures 2c and 2f). The model sensitivity analysis confirms that simulated north facing slopes remain stable for $C_v > 4.5$ kPa, which is within the range of $C_v$ values that can be expected for a pine and fir forest (Table 1), when assigned values of soil thickness and saturated hydraulic conductivity are within the interquartile range of the measured values (Figures 2c and 2f, gray lines).

Additional simulations performed on the north facing slope in the absence of apparent cohesion from vegetation demonstrate that the process of interception delays the onset of conditions that are conducive to slope failure by several hours but does not prevent the model-simulated factor of safety from falling below 1 (Figure 2). Accounting for interception reduces the total depth of water reaching the ground surface from

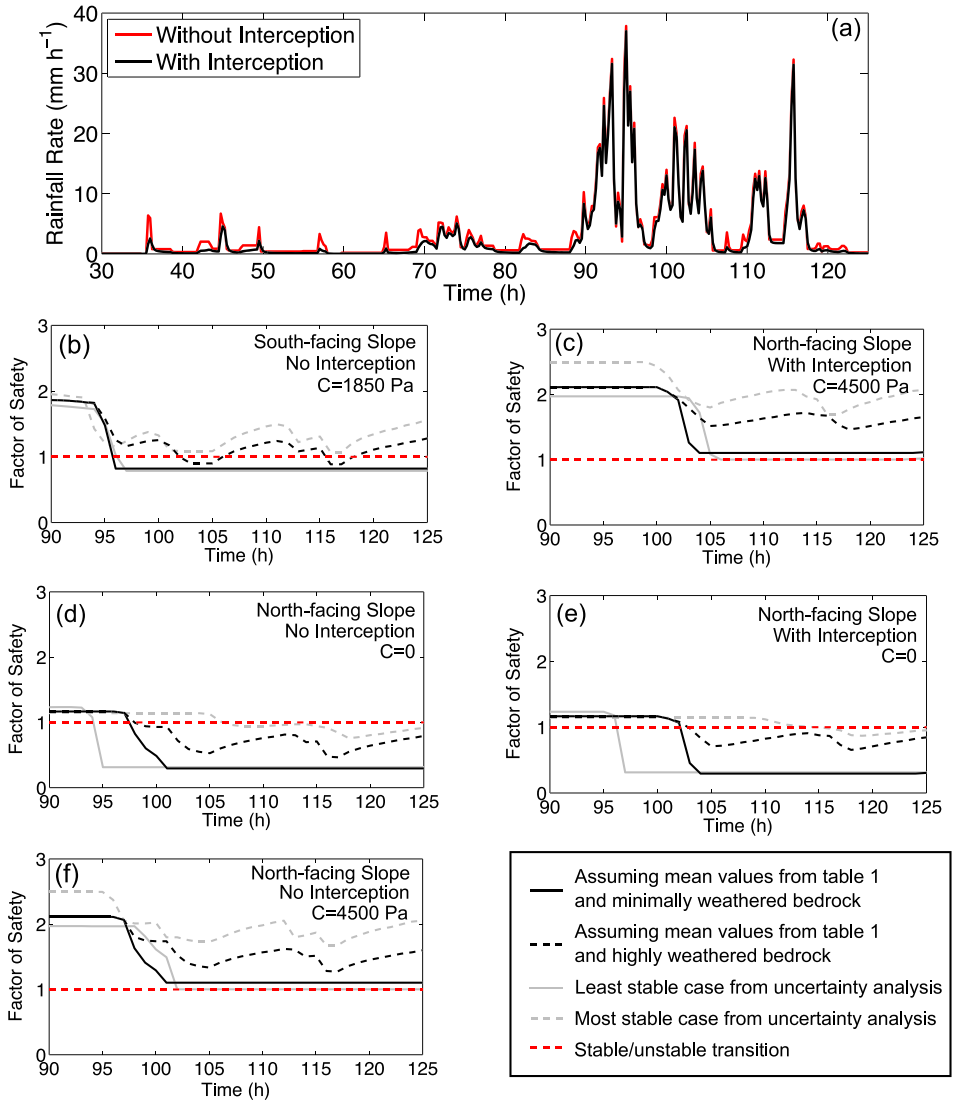


**Figure 2.** Slope stability on north and south facing hillslopes varies with time and depends on interception processes, bedrock properties, and apparent cohesion. (a) Effective rainfall rate, with and without interception, as a function of time since the start of the storm. Model-simulated factor of safety (based on the hydrologic conditions at the soil-bedrock interface) throughout the storm on north and south facing hillslopes for cases (c,e) with and (b,d, and f) without the effects of interception. There are several different solutions for each scenario. The upper black line corresponds to the case where the underlying bedrock is highly weathered and the lower black line corresponds to the case where the bedrock is not substantially weathered. Gray lines show how the factor of safety varies with soil thickness and saturated hydraulic conductivity values that are within the interquartile range of measured values.

333 mm to 283 mm. Interception substantially modifies the effective rainfall rate during portions of the storm where intensities are relatively low, but has a comparatively small influence on the effective rainfall rate when intensity is high (Figure 2a).

The role of bedrock permeability appears to be more influential than the process of interception during the studied event. High positive pore pressures dissipate slightly faster in cases where the bedrock is more weathered relative to when it is less weathered, allowing the factor of safety to slowly increase between periods of intense rainfall (Figure 2). Still, in the absence of apparent cohesion from root reinforcement, not even the combined effects of interception and a highly permeable bedrock lead to a scenario where north facing hillslopes remain stable throughout the storm (Figure 2e). North facing hillslopes do remain stable, however, as long as the apparent cohesion from root reinforcement is greater than ≈4.5 kPa. This effect is observed even in the absence of interception and the presence of bedrock with a low saturated hydraulic

conductivity (Figure 2). Numerical simulations indicate that the factor of safety on north facing hillslopes would remain greater than 1 until the hillslope angle, $\theta_t$, exceeds ≈35°. No landslides were triggered on the north facing slope in our study area at angles less than 35°; the two landslides on the north facing hillslope occurred on slopes of ≈36°–38°.

## 5. Discussion

Measurements of soil thickness and hydraulic properties at our study site demonstrate that north and south facing hillslopes have developed differently, likely as a result of microclimatic differences induced by slope aspect. However, numerical model simulations of changing pore pressure and slope stability throughout the rainstorm suggest that the measured variations in soil properties between north and south facing hillslopes at our study area are insufficient to account for the preponderance of landslide initiation locations on south facing hillslopes. More precisely, if vegetation were not a factor (i.e., no interception and no root reinforcement), model results indicate that debris flows would have been likely on both north and south facing slopes whereas extensive slope failure only occurred on the south facing hillslope (Figure 2). Our results support those of *Rengers et al.* [2016], who concluded that vegetation, and not aspect-driven variations in soil thickness or bedrock weathering, controlled slope stability during the September rainstorm.

Using the numerical model, we were also able to explore how variations in vegetation and soil thickness influenced slope stability during the studied rainstorm. Variations in rainfall interception due to a dense forest on the north facing hillslope do not appear to have substantially reduced the risk of landsliding on those slopes relative to the hypothetical scenario where no interception would have occurred (Figure 2). Canopy interception is generally most effective during small rainfall events compared to large rainfall events (e.g., *Reid and Lewis*, 2009) and is likely to have only minor impacts on slope stability during long, intense rainstorms [*Sidle and Ziegler*, 2016]. Modeling of interception and slope stability at our study area suggests similar behavior, with interception only substantially modifying the delivery of water to the soil surface during low-intensity portions of the storm (Figure 2a). As such, results may differ from those seen here in environments where landslides are triggered by rainfall intensities that are comparatively small [e.g., *Godt et al.*, 2009].

Numerical model results further indicate that the presence of more permeable bedrock on the north facing hillslope in our study area would not have reduced pore water pressure sufficiently to stabilize soil on the north facing hillslope (Figure 2). Additional reinforcement in the form of apparent cohesion provided by tree roots on the north facing hillslope, however, would be sufficient to stabilize those slopes throughout the storm (Figure 2). Furthermore, model sensitivity analyses indicate that soils on south facing slopes would have become unstable for a range of assigned thicknesses and saturated hydraulic conductivity values (Figure 2f). Therefore, while differences in soil thickness may have played a role in determining slope failure locations, it is unlikely that variations in soil thickness alone were sufficient to explain the observed increased frequency of landslides on south facing hillslopes. We attribute the overall stability of north facing hillslopes relative to south facing hillslopes at our study area to be the result of apparent cohesion supplied by the dense pine and fir forest. More generally, since the model-simulated factor of safety is far less sensitive to variations in interception and bedrock permeability than to changes in apparent cohesion and *Rengers et al.* [2016] demonstrated a link between areas of low vegetation density and landslide locations, results suggest that spatial variations in root reinforcement were responsible for controlling the observed spatial pattern in landslide initiation locations throughout the Colorado Front Range.

Incorporation of apparent root cohesion into a one-dimensional infinite slope stability analysis is complicated by the assumptions required to transform the stabilizing effects of a three-dimensional root network into an equivalent basal shear stress [e.g., *Lu and Godt*, 2013]. In this study, we base our choice of $C_v$ on prior studies [*Gray and Megahan*, 1981; *Schmidt et al.*, 2001], but acknowledge that any one-dimensional framework for quantifying the geomechanical effects of roots on slope stability may introduce more uncertainty relative to the framework used to model the hydrologic effects of vegetation. Most importantly for the purposes of this study, however, spatial variations in interception, soil thickness, and bedrock permeability can be reasonably ruled out as being the controlling factor on the spatial distribution of landslides within our study area. Given that variations in apparent root cohesion between north and south facing slopes are of the proper magnitude to generate the observed aspect dependence on debris flow initiation locations (Figure 2), apparent root cohesion provides the most likely explanation for the stability of north facing slopes relative to south facing slopes.

While root reinforcement and its effects on slope stability, assuming other factors remain unchanged, are well established [e.g., *Wu et al.*, 1979; *Gray and Megahan*, 1981; *Schmidt et al.*, 2001; *Roering et al.*, 2003], direct comparisons between the stability of forested and unforested slopes are complicated in many natural settings by the coevolution of vegetation and soil properties. Since vegetation provides slope stability through root reinforcement and both soil properties and vegetation can influence hydrologic processes, it is difficult to isolate the importance of the geomechanical effects of vegetation relative to its hydrologic effects when assessing landslide susceptibility on a regional scale. However, evaluating the importance of the geomechanical effects of vegetation on slope stability relative to its hydrologic effects has important implications for developing robust assessments of how landslide hazards will change in response to disturbance events and different climate scenarios. Because the vegetation properties that determine the effectiveness of interception (e.g., canopy storage and drip rate) are not directly related to the factors that determine the magnitude of root reinforcement (e.g., root density and diameter), it is possible for a conversion in vegetation type to modify the typical magnitudes of canopy interception and root reinforcement in different, and perhaps opposite, ways. Moreover, a change in canopy cover reduces interception immediately following a severe wildfire whereas root reinforcement may change over longer timescales of years to decades following such disturbance events [*Schmidt et al.*, 2001; *Jackson and Roering*, 2009].

Our analysis suggests that the root reinforcement provided by vegetation on north facing hillslopes was primarily responsible for stabilizing soil on those slopes, which led to a dramatic disparity in debris flow initiation between north and south facing slopes during the September 2013 rainfall event, whereas the impact of vegetation on slope stability through its effects on interception and bedrock permeability were comparatively minor. While present-day vegetation patterns in the Colorado Front Range, and throughout much of the semiarid southwestern U.S., currently overlie a landscape where soil development and bedrock weathering (both of which affect slope stability) have developed over much longer time scales, our analysis suggests landslide susceptibility is primarily governed by the local, geomechanical effects of vegetation during extreme rainfall events. Therefore, regional scale analyses of slope stability that aim to predict the spatial distribution of landslides throughout the landscape could be substantially improved by characterizing spatial variations in vegetation type and density. Additionally, evaluations of landslide hazards under future climate change scenarios should account for associated changes in vegetation communities, particularly with respect to how they may influence root reinforcement.

## 6. Conclusions

Aspect-driven variations in vegetation type and density within the Colorado Front Range allowed for a detailed study of the role of vegetation in controlling landslide initiation during an extreme rainfall event. We analyzed the relative importance of different interactions among vegetation, subsurface hydrology, and slope stability using a combination of direct field measurements, laboratory analyses, and numerical modeling. Numerical model results indicate that apparent cohesion provided by the root network was the primary reason for the stability of north facing slopes relative to south facing slopes. Results highlight the importance of root reinforcement relative to other factors that may also be influenced by the presence of vegetation, such as interception and bedrock permeability, during extreme rainfall events. Further, results suggest that future landslide hazards throughout water-limited portions of the western U.S. may be particularly sensitive to anticipated perturbations in forest structure as a result of climate change.

**Acknowledgments**
We thank Georgina Bennett and an anonymous reviewer for helpful comments that improved the quality of the manuscript. All data used in this paper are available upon request. This work was supported by the U.S. Geological Survey (USGS) Landslide Hazards Program. Any use of trade, product, or firm names is for descriptive purposes only and does not imply endorsement by the U.S. Government.

## References

Befus, K., A. Sheehan, M. Leopold, S. Anderson, and R. Anderson (2011), Seismic constraints on critical zone architecture, Boulder Creek watershed, Front Range, Colorado, *Vadose Zone J.*, *10*(3), 915–927.

Birkeland, P., R. Shroba, S. Burns, A. Price, and P. Tonkin (2003), Integrating soils and geomorphology in mountains—An example from the Front Range of Colorado, *Geomorphology*, *55*(1), 329–344.

Burnett, B. N., G. A. Meyer, and L. D. McFadden (2008), Aspect-related microclimatic influences on slope forms and processes, Northeastern Arizona, *J. Geophys. Res.*, *113*, F03002, doi:10.1029/2007JF000789.

Carsel, R. F., and R. S. Parrish (1988), Developing joint probability distributions of soil water retention characteristics, *Water Resour. Res.*, *24*(5), 755–769.

Coe, J. A., J. W. Kean, J. W. Godt, R. L. Baum, E. S. Jones, D. J. Gochis, and G. S. Anderson (2014), New insights into debris-flow hazards from an extraordinary event in the Colorado Front Range, *GSA Today*, *24*, 4–10.

Ebel, B. A., F. K. Rengers, and G. E. Tucker (2015), Aspect-dependent soil saturation and insight into debris-flow initiation during extreme rainfall in the Colorado Front Range, *Geology*, *43*(8), 659–662.

Gabet, E. J., and T. Dunne (2002), Landslides on coastal sage-scrub and grassland hillslopes in a severe El Niño winter: The effects of vegetation conversion on sediment delivery, *Geol. Soc. Am. Bull.*, *114*(8), 983–990.

Godt, J. W., R. L. Baum, and N. Lu (2009), Landsliding in partially saturated materials, *Geophys. Res. Lett.*, *36*, L02403, doi:10.1029/2008GL035996.

Gray, D. H., and W. F. Megahan (1981), Forest vegetation removal and slope stability in the Idaho batholith, *USDA For. Serv. Res. Pap. INT (USA). No. 271*, U.S. Dept. of Agric., For. Serv., Intermountain Forest and Range Exp. Station, Ogden, Utah.

Green, G. N. (1992), The digital geologic map of Colorado in ARC/INFO format, *U.S. Geol. Surv. Open-File Rep. 92-0507*, U.S. Geol. Surv., Denver, Colo.

Jackson, M., and J. Roering (2009), Post-fire geomorphic response in steep, forested landscapes: Oregon Coast Range, USA, *Quat. Sci. Rev.*, *28*, 1131–1146.

Katsura, S., K. Kosugi, T. Mizutani, and T. Mizuyama (2009), Hydraulic properties of variously weathered granitic bedrock in headwater catchments, *Vadose Zone J.*, *8*(3), 557–573.

Keim, R. F., and A. E. Skaugset (2003), Modelling effects of forest canopies on slope stability, *Hydrol. Processes*, *17*(7), 1457–1467.

Lu, N., and J. Godt (2008), Infinite slope stability under steady unsaturated seepage conditions, *Water Resour. Res.*, *44*, W11404, doi:10.1029/2008WR006976.

Lu, N., and J. W. Godt (2013), *Hillslope Hydrology and Stability*, Cambridge Univ. Press, Cambridge, U. K.

Marr, J. W. (1961), *Ecosystems of the East Slope of the Front Range in Colorado*, Univ. of Colorado Press, Boulder, Colo.

Rech, J. A., R. W. Reeves, and D. M. Hendricks (2001), The influence of slope aspect on soil weathering processes in the Springerville volcanic field, Arizona, *Catena*, *43*(1), 49–62.

Reid, L. M., and J. Lewis (2009), Rates, timing, and mechanisms of rainfall interception loss in a coastal redwood forest, *J. Hydrol.*, *375*(3), 459–470.

Rengers, F., L. McGuire, J. Coe, J. Kean, R. Baum, D. Staley, and J. Godt (2016), The influence of vegetation on debris-flow initiation during extreme rainfall in the northern Colorado Front Range, *Geology*, *4*, doi:10.1130/G38096.1.

Roering, J. J., K. M. Schmidt, J. D. Stock, W. E. Dietrich, and D. R. Montgomery (2003), Shallow landsliding, root reinforcement, and the spatial distribution of trees in the Oregon Coast Range, *Can. Geotech. J.*, *40*(2), 237–253.

Rutter, A., K. Kershaw, P. Robins, and A. Morton (1972), A predictive model of rainfall interception in forests, 1. Derivation of the model from observations in a plantation of Corsican pine, *Agric. Meteorol.*, *9*, 367–384.

Rutter, A., A. Morton, and P. Robins (1975), A predictive model of rainfall interception in forests. II. Generalization of the model and comparison with observations in some coniferous and hardwood stands, *J. Appl. Ecol.*, *12*, 367–380.

Schmidt, K., J. Roering, J. Stock, W. Dietrich, D. Montgomery, and T. Schaub (2001), The variability of root cohesion as an influence on shallow landslide susceptibility in the Oregon Coast Range, *Can. Geotech. J.*, *38*(5), 995–1024.

Sidle, R. C., and A. D. Ziegler (2016), The canopy interception-landslide initiation conundrum: Insight from a tropical secondary forest in northern Thailand, *Hydrol. Earth Syst. Sci. Discuss.*, doi:10.5194/hess-2016-96.

Šimunek, J., M. T. van Genuchten, and M. Sejna (2005), *The Hydrus-1d Software Package for Simulating the Movement of Water, Heat, and Multiple Solutes in Variably Saturated Media*, Univ. of California, Riverside, Calif.

Teklehaimanot, Z., and P. Jarvis (1991), Direct measurement of evaporation of intercepted water from forest canopies, *J. Appl. Ecol.*, *28*, 603–618.

Veblen, T. T., and J. A. Donnegan (2005), *Historical Range of Variability for Forest Vegetation of the National Forests of the Colorado Front Range*, USDA For. Serv., Rocky Mountain Region.

Wilkinson, P., M. Anderson, and D. Lloyd (2002), An integrated hydrological model for rain-induced landslide prediction, *Earth Surf. Processes Landforms*, *27*(12), 1285–1297.

Williams, A. P., et al. (2013), Temperature as a potent driver of regional forest drought stress and tree mortality, *Nat. Clim. Change*, *3*(3), 292–297.

Wu, T. H., W. P. McKinnell III, and D. N. Swanston (1979), Strength of tree roots and landslides on Prince of Wales Island, Alaska, *Can. Geotech. J.*, *16*(1), 19–33.

Zhang, R. (1997), Determination of soil sorptivity and hydraulic conductivity from the disk infiltrometer, *Soil Sci. Soc. Am. J.*, *61*(4), 1024–1030.